Natural Resources for Human Health

eISSN: 2583-1194

Original Research

Received 30 May 2026
Revised 20 June 2026
Accepted 18 July 2026

Natural Resources for Human Health 2026, Vol. 6 (10s): 598–613

KEYWORDS:
Fruit peel waste, Activated carbon, ACG dye, Adsorption, Kinetic, isotherm.

Sustainable Biomass-derived Activated Carbons for the Adsorptive Removal of Alizarin Cyanine Green Dye: Isotherm, Kinetic and Comparative Performance with Commercial Activated Carbon

M. Maheswari[1], P. Muthirulan[2*], C. Starlin Kamala[3]

[1]Research Scholar (Reg. No. 22223282032006), Department of Chemistry, Women's Christian College (affiliated to Manonmaniam Sundaranar University, Tirunelveli-627012), Nagercoil – 629001, TN, India
[2]Department of Chemistry, Lekshmipuram College of Arts and Science (affiliated to Manonmaniam Sundaranar University, Tirunelveli-627012), Neyyoor-629802, TN, India
[3]Research Scholar (Reg. No. 22223282032006), Department of Chemistry, Women's Christian College (affiliated to Manonmaniam Sundaranar University, Tirunelveli-627012), Nagercoil – 629001, TN, India
*Email: pmuthirulan@gmail.comn

ABSTRACT: Activated carbons derived from four fruit peel wastes—Soursop Fruit Peel Carbon (SFPC) and Wild Jack Fruit Peel Carbon (WFPC)—were synthesized and evaluated as sustainable adsorbents for the removal of Alizarin Cyanine Green dye from aqueous solutions. The physicochemical characteristics of the prepared carbons were examined. XRD analysis indicated the presence of graphite-like amorphous structures. FTIR spectra confirmed the presence of various surface functional groups, including C = C, C = O, C–H, C–C, and C–O. TGA-DTA and SEM confirming their thermal stability with well-developed porous surface texture. Batch adsorption experiments were performed to investigate the influence of operational parameters on dye uptake. The Langmuir isotherm model provided the best fit for the equilibrium data, indicating a maximum adsorption capacity of 576.92, 398.60 and 389.36mgg-1 for CAC, SFPC and WFPC. Kinetic analyses revealed that dye adsorption followed the pseudo-second-order model, suggesting chemisorption as the dominant mechanism. These findings demonstrate that widely available and low-cost fruit peel wastes can serve as effective, environmentally friendly, and sustainable precursors for the production of activated carbon towards environmental sustainability.

1. INTRODUCTION

Rapid industrial growth, particularly in textile, paper, leather, and dye-manufacturing sectors, has resulted in the continuous discharge of highly colored effluents into natural water bodies. Synthetic dyes are designed to resist degradation, making them persistent, toxic, and difficult to remove using conventional treatment methods. Among various dyes, Malachite Green (MG) is one of the most widely used cationic dyes in textile processing, paper production, and biological staining. Although MG is not considered highly hazardous at very low concentrations, prolonged exposure or elevated levels can cause severe health effects including eye irritation, nausea, respiratory complications, and oxidative stress. Its strong color, high solubility, and resistance to biodegradation make MG a persistent pollutant in aquatic environments, necessitating the development of efficient removal methods. Their presence even at very low concentrations reduces light penetration, inhibits photosynthesis, disrupts aquatic ecosystems, and poses serious risks to human health. Therefore, the development of efficient, sustainable, and low-cost adsorption materials for dye-laden wastewater treatment has become an urgent environmental priority [1,2].

Conventional wastewater treatment methods, including coagulation–flocculation, chemical oxidation, and biological degradation, often exhibit limited efficiency for dye removal because of the complex aromatic structures and chemical stability of most dyes [3]. In this context, adsorption-based technologies have emerged as a highly efficient and versatile approach to remove both cationic and anionic dyes from aqueous media. Activated carbon is widely recognized as an effective adsorbent due to its high surface area, tunable pore structure, and abundant active sites [4]. However, commercial activated carbon remains expensive, and its large-scale use is often limited in developing regions. This challenge has encouraged researchers to explore renewable, low-cost, and locally available biomass residues as alternative precursors for activated carbon production [5]. Among various adsorbents, activated carbons prepared from fruit-peel wastes have attracted significant attention owing to their abundance, low cost, renewable nature, and excellent physicochemical properties. Fruit-processing industries generate large volumes of peel residues such as soursop, jackfruit, rambutan, mangosteen, orange, banana, and pomegranate peels, which contain lignocellulosic components ideal for carbonization and activation Fruit peels represent one of the most abundant agro-waste materials generated worldwide. They are rich in lignocellulosic components such as cellulose, hemicellulose, and lignin, which make them suitable precursors for producing highly porous activated carbon. Valorizing fruit-peel wastes into activated carbon not only reduces solid-waste disposal issues but also contributes to circular-economy practices by converting agricultural residues into value-added adsorbents [6,7]. Recent studies have demonstrated that fruit-peel-derived activated carbon exhibits excellent adsorption performance for various organic pollutants, particularly synthetic dyes, due to its well-developed porosity, surface functional groups, and enhanced affinity toward dye molecules [8-10].

The work aims to explore the adsorption characteristics, efficiency, and applicability of fruit-peel-derived activated carbon as a sustainable and cost-effective alternative to conventional adsorbents for wastewater treatment. The findings aim to contribute to green wastewater treatment technologies and promote the utilization of agro-waste materials for environmental remediation.

2. MATERIALS AND METHODS

2.1 Chemicals and Reagents

Alizarin Cyanine Green dye was purchased from Sigma–Aldrich used as received. The physico-chemical characteristics, application, toxicity and chemical structure of ACG dye is listed in Table 1. All the other chemicals are analytical grade and utilized in their unpurified as-received state. All experiments were done at room temperature, and double-distilled (DD) water was used throughout the investigation.

Dye	**Alizarin Cyanin Green**
CI No.	61570
Characteristics	Anionic, water soluble, Green Colour
Formula	$C_{28}H_{20}N_2Na_2O_8S_2$;MW : 623
Structure	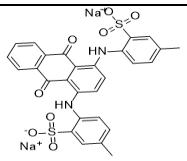
λ_{max}	519 nm
Applications	It can be used to dye paper, chromed leather, wool, silk, and nylon (acid bath), to stain wood, and to color anodized aluminum, urea-melamine resin, and soap.

2.2 Preparation, Activation and Storage of Adsorbent

Peels of Soursop Fruit (SFP) and Wild Jack Fruit (WFP) were collected from local farms and shop nearby our college campus; then the fruit peels are sliced into little pieces and water-cleaned prior to use. It is then dried and carbonized in a muffle furnace at a temperature of 300-400°C. Afterward, the carbonized materials were activated with 200g of carbon and

600 ml 4N nitric solution for 120 minutes at 80°C. Next, it was rinsed multiple times with boiling DD water to remove any acid (tested using pH Paper) and metal ions. The activated adsorbent was then dried in an oven at 120°C for 5hr. It was then placed in a sealed wide-mouth laboratory bottle and used to conduct absorption findings. The adsorbents employed in the present work were labeled as Soursop Fruit Peel Carbon (SFPC), Wild Jack Fruit Peel Carbon (WFPC) and Commercial Activated Carbon (CAC) [11-13].

2.3 Instrumental Studies

The as-prepared SFPC and WFPC adsorbents were ground and sieved using a Jayanth brand (India) mechanical sieve. This produced consistent, discrete particles of different sizes (90 microns). Systronics digital pH monitor (model: 335) was used to measure pH. The FTIR spectra of the adsorbent material were obtained in KBr pellets using a Spectrometer (Model BIORAD WIN IR). SEM photographs of the adsorbent material were taken by JEOL Instrument (Model JSM – 5300).

2.4 Batch Adsorption Experiments

The adsorption experiments were carried out in a batch process. Adsorption experiments were carried out by adding a fixed amount of adsorbents into 250mL stopper flasks containing a definite volume (100 ml in each case) of different initial concentrations of dye solution at room temperature (30□ 1□ C). The flasks were placed in a mechanical shaker and agitation was provided at 130 rpm for required time to ensure equilibrium was reached. At time t = 0 and equilibrium, the absorbance of dye solution was determined by the photo colorimeter, at λmax (498nm) value of dye. The amount of adsorption at equilibrium, qe (mg/g), was calculated by

Amount adsorbed (qe) = (Ci-Ce) / m (1)

Where, Ci and Ce were the initial and equilibrium concentration (in mgl-1 or ppm) of dye, respectively and m is the weight of AC (in gl-1). The dye removal percentage can be calculated as follows:

Percentage removal = 100 (Ci-Ce) / Ci (2)

The effect of dose of SFPC and EFPC adsorbents on the amount of ACG dye adsorbed was obtained by adding different amounts of adsorbents by keeping other parameters as constant. In order to study the kinetics/dynamics of adsorption of dyes, the adsorption experiments were conducted by varying the contact time (range: 5 – 60 min.) at fixed optimum initial concentration of dyes with a fixed dose of adsorbent and solution pH. The dye concentrations were measured at different time intervals [11-13]. orem ipsum dolor sit amet, consectetur adipiscing elit. Fusce lacinia arcu et nulla. Nulla vitae mauris non felis mollis faucibus.

3. RESULTS AND DISCUSSION

3.1 Preliminary Analysis

3.1 Physico-Chemical Properties of ACs

The physico-chemical properties such as bulk density, moisture content, loss on ignition (LOI), residue after ignition, pH, electrical conductivity, zeropoint charge (pH $_{ZPC}$), surface area (by acetic acid method), decolourising power (methylene blue number) and phenol number of CAC and indigenously prepared ACs(SFPC, WFPC, RFPC and MFPC) have been determined. The physico-chemical characteristics of CAC and indigenously prepared ACs are given in Table 2.

Table 2 Physico – chemical characteristics of CAC and indigenously prepared ACs

Property	CAC	MFPC	RFPC	WFPC	SFPC
Bulk density(gmL^{-1})	0.964	0.747	0.573	0.785	0.906
Moisturecontent (%)	10.1*	1.65	1.95	2.18	1.87
Loss on ignition (%)	95.0*	27.5	25.2	59.1	61.8
Residue after ignition(%)	5.0	72.5	74.8	40.9	38.2

pH	9.4	8.9	8.7	9.0	9.2
Zero point charge(pH_{ZPC})	7.25	4.10	4.50	4.20	7.10
Surface area(m^2g^{-1})	875	730	692	765	787
Decolourising power (mgg^{-1})	12.0	8.1	5.5	8.5	10.0
Phenol number x 10^{-3} (mgl^{-1})	8.35	8.75	9.20	8.85	8.70

* Data reported by Emerck, India are close to experimental values.

The bulk density of CAC is very high and BDC is very low among these ACs. The indigenously prepared ACs possess lesser bulk density than that of CAC and among the indigenously prepared ACs, SC has the maximum value of bulk density. The lower moisture content of the indigenously prepared ACs (range = 0 - 2%) is mainly due to its method of preparation *viz*., high temperature employed during carbonisation/pyrolysis and activation.The moisture content though does not affect the adsorptive power, it dilutes the adsorbent and therefore necessitates the use of additional amount of adsorbent (if moisture content is high and adsorptive capacity is low) for the water treatment process [11-13].

The LOI of CAC is found to be very high and it has also reported to be 95 % (based on its residue after ignition at 600°C = 5 %) by E Merck, India. This may be probably due to high mineral content and greater extent of char formation during ignition, especially in the case of indigenously prepared ACs. This fact is also confirmed by the higher values of residue left after ignition, in the case of indigenously prepared ACs than that of CAC. The values of residue obtained after the ignition of indigenously prepared ACs are higher, than that of CAC (5.0 %). This is also due to the presence of higher content of refractories and minerals and greater extent of char formation during thermal degradation. ACs and CAC are found to be alkaline and basic in nature (pH = 8.6–9.4) [14].

The zero point charge (pH_{ZPC}) of CAC is 7.25, while the values of pH_{ZPC} of ACs are lesser than that of CAC. Although the pH_{ZPC} of some of the carbons are nearly neutral, the values for most of the ACs are in the mild acidic pH range. This may probably be due to the presence of surface functional groups like- OH,- COOH etc. which are slightly acidic in nature. The surface area (determined by acetic acid method) of the carbonaceous adsorbents is of the order of 663 – 875 $m^2 g^{-1}$.Among the indigenously prepared ACs, SFPC possess the maximum surface area and RFPC has the minimum surface area. The observed increasing order of the surface area of ACs is: **WFPC<SFPC<CAC**

Adsorbent with high surface area will possess the higher decolourising power (methylene blue (MB) number) and lower phenol number. The higher decolourising power and lower phenol number of CAC and SFPC, compared to other ACs may be attributed due to the larger surface area of these ACs. To sum up, among the indigenously prepared ACs, RFPC is less porous with low surface area, while MFPC, WFPC and SFPC possess high porosity and high surface area [15].

3.2 XRD studies of fruit peel based biomass derived activated carbons

To identify the kind of developed carbon materials (SFPC and WFPC) made from peel wastes and its crystalline structure, powdered X-ray powder diffraction was used. The biomass derived activated carbon (SFPC and WFPC) produced from peel wastes were evidently created in an amorphous condition, according to XRD measurements (Figure 1). The XRD spectra of all the four carbons viz., SFPC, WFPC, MFPC and RFPC showed two broad obvious, unique diffraction peaks at 2θ of approximately 25° and 40°, respectively, which correspond to the planes (002) and (101), suggesting that the material is amorphous and that the majority of it is made up of carbon skeleton basis. Acid activation breaks the crystalline phase of high content cellulose, forming amorphous carbon. There are no appreciable differences between SFPC and WFPC that are produced during the carbonization and dehydration processes. The XRD pattern closely resembles the previously published research work [12,13,16].

Natural Resources for Human Health
eISSN: 2583-1194

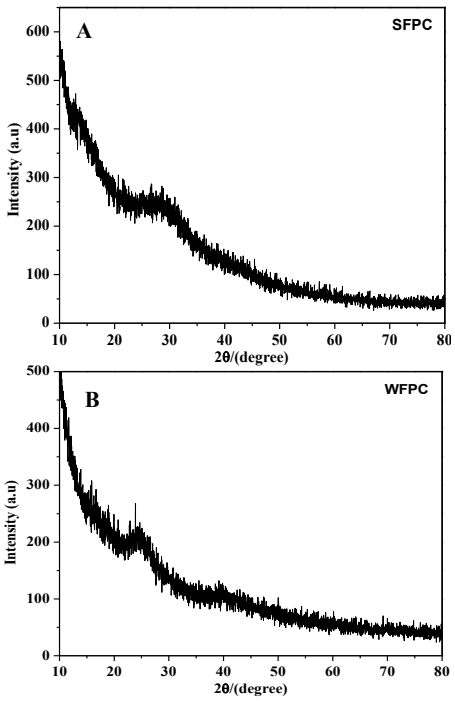

Figure 1 XRD images of (A) Soursop Fruit Peel Carbon and (A) Wild Jack Fruit Peel Carbon

3.3 Thermogravimetry Analysis of fruit peel based biomass derived activated carbons

The thermogravimetric analysis, abbreviated as TGA, has been carried out and is depicted in Figure 2, in order to determine how temperature affects the physical nature of the IPA carbon materials that are derived from fruit peel biomass wastes. It is clear from looking at the figure that the initial or first weight loss that occurs around 100–300°C is somewhere in the range of 8–15%. This loss is primarily attributed to the loss of moisture, volatile compounds, impurities, and absorbed water that are present on the surface of the adsorbent [17].

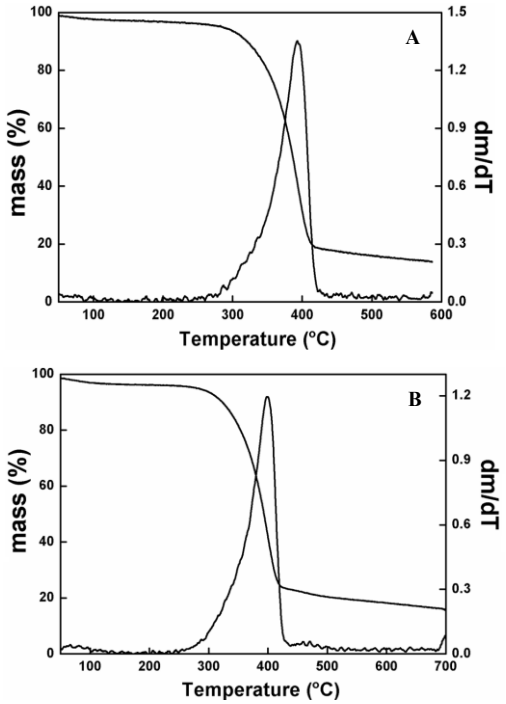

Figure 2 TGA-DTA Spectra of (A) Soursop Fruit Peel Carbon and (A) Wild Jack Fruit Peel Carbon

In addition, the second substantial weight loss that occurs about 300°C and continues up to 410°C may be attributed to the removal of oxygen-containing functional groups as well as the dissolution of other functional groups. Moreover, after 410 °C, there is a loss of weight, which indicates the structural decomposition of the activated carbon back bone skeleton. Moreover, the DTA graph of IPACs showed one acute exothermic peak at roughly 100°C, suggesting dehydroxylation of the carbon, followed by one broad endothermic peak representing the desorption of water molecules around 50-90°C. Later on, two tiny exothermic was also seen at 486°C and 626°C, which was followed by one broad endothermic peak at 800-600°C. This signifies a steady decline of the base carbon material, which was ascribed to the multistep decomposition behavior of the SFPC carbon material [12,13, 18].

3.4 Impact of dye solution concentration on ACG dye removal by CAC, SFPC, and WFPC adsorbents

The uptake of Alizarin cyanine green over the adsorbents CAC, SFPC, and WFPC was investigated at different ranges of initial concentration, keeping contact time, dose of adsorbent, initial pH, and particle size fixed. The results are compared and graphically shown in Figure 3.

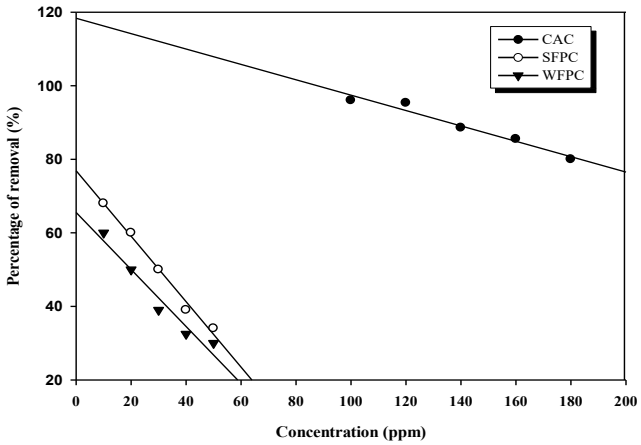

Figure 3 Effect of initial concentration for the removal of ACG dye due to the adsorption on CAC and IPACs [Contact time = 30 min; pH = 7.5 for CAC, 6.5 for SFPC and WFPC; Dose = 2 gL^{-1} for CAC and 20 gL^{-1} for SFPC and WFPC; Particle size = 90 micron; agitation speed -200rpm and pH is solution pH]

The result of this experiment reveals that as concentration increases, the percentage of dye removed drops exponentially. It is also observed that at lower concentrations, the rate of elimination accelerates. This suggests that there is a decrease in the solute adsorption that occurs immediately because there aren't enough active sites available to support a high initial dye concentration. The observation might be explained by the concept that dye molecules must first meet the boundary layer during the adsorption process, then diffuse from the boundary layer film onto the biomass-derived carbon (adsorbent) surface, and finally diffuse into the adsorbent's porous surface [19,20].

3.4.1 Adsorption Isotherms

Adsorption isotherms provide information on the adsorbate's adsorption uptake behavior on the adsorbent surface. This sheds light on the forces of attraction and the affinity between the adsorbate and the sorbent surface. However, it offers a necessary situation for the production of monolayers and multilayers on the absorbent surface. Furthermore, adsorbate adsorption on the adsorbent surface might result in the creation of a single molecular layer or, if adsorbate adsorption is permitted on the surface, the accumulation of multilayer. The most often used models to study the adsorption mechanisms are the Langmuir and Freundlich isotherm models. At the molecular level, each of the isotherm models has a unique sorption mechanism [11-13]. The adsorption data were fitted with Freundlich adsorption isotherm as shown below,

$$log\left(\frac{x}{m}\right) = logk + \frac{1}{n} logC_e \quad (3)$$

.A graph plotted between log C_e against log x/m is shown in the Figure 4A.

Natural Resources for Human Health
eISSN: 2583-1194

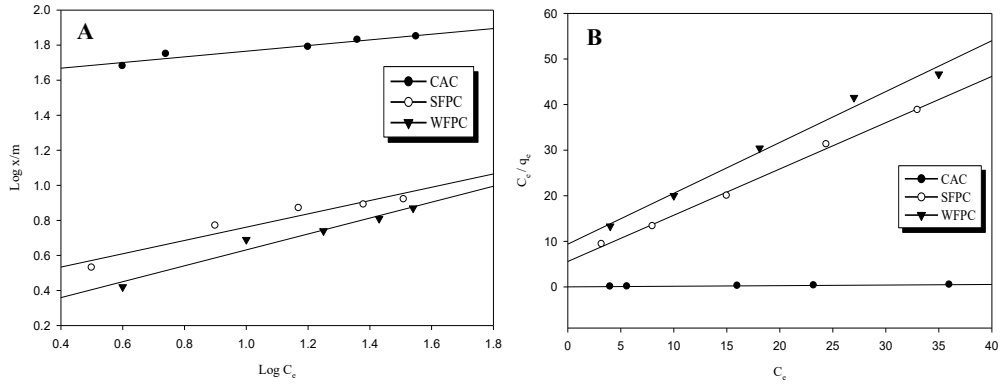

Figure 4 (A) Freundlich and (B) Langmuir adsorption isotherms for the removal of ACG dye by adsorption on CAC, SFSC and WFPC

The graph's linearity suggests that the Freundlich isotherm can be applied to the data collected during experiments. The datas of 'k' and 'n' are determined using the straight line's intercept and slope [21].

According to the Langmuir model, monolayer adsorption causes adsorbate ion adsorption on the homogenous surface. The Langmuir isotherm equation is expressed as follows,

$$C_e/q_e = 1/Q_0b + C_e/Q_o \quad (4)$$

The graph plotted between C_e/q_e against C_e is shown in the Figure 4B. From the straight line slope and intercept of the plot, the Langmuir constants Qo (mgg^{-1}) and b (Lmg^{-1}), which are associated with the adsorption energy and capacity, may be found. The correlation analysis of Freundlich and Langmuir isotherms are presented in Table 3. Correlation coefficient (r), is used to compare the isotherm equation's applicability. The findings show that the Langmuir isotherm fits data better than the Freundlich model, supporting the monolayer adsorption theory [22].

Table 3 Results of various adsorption isotherms parameters on the removal ACG dye on CAC, SFPC and WFPC adsorbents

Isotherm	**CAC**	**SFPC**	**WFPC**
Freundlich			
Slope (1/n)	0.161	0.381	0.403
Intercept (Log k)	1.604	0.379	0.245
Correlation coefficient (r)	0.931	0.926	0.976
Langmuir			
Intercept ($1/Q_ob$)	0.032	5.603	9.4
Correlation coefficient (r)	0.997	0.996	0.989
Q_o (mgg^{-1})	576.92	398.60	389.36
b ($L\ mg^{-1}$)	0.406	0.180	0.118
R_L	0.012	0.020	0.027

Additionally, favorable or unfavorable adsorption by a dimensionless parameter R_L is found using the Langmuir constants.

$$R_L = 1/ (1 + bC_0) \quad (5)$$

The isotherm might be advantageous, linear, or unfavorable depending on the value of R_L. R_L=1 is Linear, $0<R_L<1$ is Favorable, R_L=0 is Irreversible and RL>1 is Unfavorable. In certain circumstances, the R_L value is < 1. Thus, the

adsorption's nature is favorable. The sorption ability is indicated by another Langmuir constant, Q_0 and the monolayer adsorption capacity of adsorbents is in the order **WFPC<SFPC<<<CAC.**

3.5 Impact of agitation time for the elimination of ACG dye on CAC, SFPC, and WFPC adsorbents

To find out the maximum adsorption equilibrium time, the color elimination or % removal of Alizarin cyanine green on CAC, SFPC, and WFPC has been examined by varying agitation time. Adsorption tests were conducted at various contact times, using the dye's optimal beginning concentration and initial pH of the dye solution, weight of the biomass carbon, and size of adsorbent particle kept constant. The percentage removal plot was shown in the Figure 5. The adsorption process increases with increasing contact time.

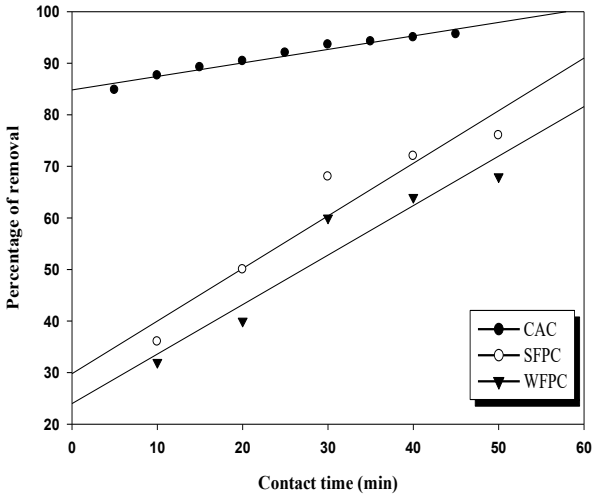

Figure 5 The effect of contact duration on the removal of ACG dye by CAC, SFPC and WFPC adsorbents [Initial concentration = 100 ppm for CAC, 10 ppm SFPC and WFPC; Dose = 2 gL^{-1} for CAC, 20 gL^{-1} for SFPC and WFPC; pH = 7.5 for CAC and 6.5 for SFPC and WFPC; Particle size = 90 micron; Varying contact time from 10 to 60 minutes, agitation speed -200rpm]

The % removal of ACG dye molecule increases with increasing the agitation time [23-25].

3.5.1 Kinetic Modeling

The rate of the adsorption process is ascertained using the kinetic models. For the kinetic study of the adsorption process under consideration, the following first–order kinetic equations Natarajan and Khalaf, Lagergren, Bhattacharya and Venkobachar were employed.

First ordr equation : $(1/q_t) = (k/q_{max})(1/t) + (1/q_{max})$ (6)

Natarajan and Khalaf equation : $\log(C_i / C_t) = (k / 2.303) t$ (7)

Lagergren equation : $\log(q_e-q_t) = \log q_e - (k_{ad}/2.303) t$ (8)

Bhattacharya and Venkobachar : $\log [1-U(t)] = -(k_{ad} / 2.303) t$ (9)

where, C_i and C_t are respectively, the concentration of dye (in ppm) at time zero and at time t; q_e and q_t are the amount of dye adsorbed per unit mass of the adsorbent (in mg g^{-1}), respectively at equilibrium time and at time t, and q_{max} is the maximum adsorption capacity (in mg g^{-1}), k and k_{ad} are the adsorption rate constants (in $min.^{-1}$) and $U(t) = [(C_i - C_t)] / (C_i – C_e)]$; C_e = concentration of dye (in ppm) at equilibrium (optimum) contact time . The linear graphical plots between the values of (i) $1/q_t$ and $1/t$, (ii)$\log (C_i / C_t)$ and time,(iii) $\log (q_e-q_t)$ and time and (iv) $\log [1-U(t)]$ and time, indicate the applicability of the above kinetic equations, and the first order nature of the adsorption process.

Natural Resources for Human Health
eISSN: 2583-1194

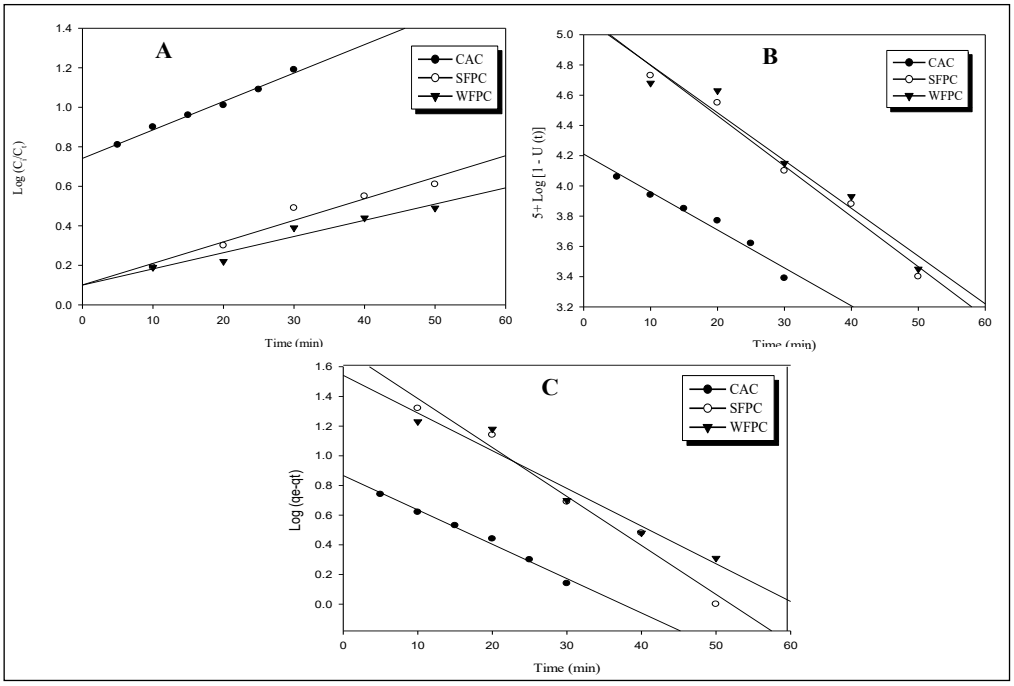

Figure 6 (A) Natrajan and Khalaf plot; (B) Bhattacharya and Venkobachar plot and (C) Lagergren plot for ACG dye removal by adsorption on CAC, SFPC and WFPC

Table 4 Adsorption kinetic experimental parameters on the removal ACG dye on CAC, SFPC and WFPC adsorbents

Parameters	**CAC**	**SFPC**	**WFPC**
Natarajan and Khalaf Equation			
Correlation coefficient (r)	0.989	0.951	0.937
k (min^{-1})	0.032	0.023	0.018
Bhattacharyaand Venkobachar Equation			
Correlation coefficient (r)	0.961	0.979	0.952
k (min^{-1})	0.057	0.075	0.071
Lagergren Equation			
Correlation coefficient (r)	0.993	0.979	0.951
k (min^{-1})	0.048	0.075	0.057
Intra-particle diffusion Equation			
Correlation coefficient r	0.995	0.956	0.919
k	1.207	0.053	0.045
Intercept C	39.87	0.017	0.026

The intra-particle diffusion process is often the rate - limiting step in many adsorption processes. The intra-particle diffusion model is given by the equation :

$q_t = k_p t^{1/2} + c$ (10)

Where, q_t is the amount of dye adsorbed (in mgg^{-1}) at time t; and c and k_p are the intercept and intra-particle diffusion rate constant (unit:mg g^{-1} $min^{0.5}$), respectively. The value of intercept(c), give an idea about boundary layer thickness, *i.e.*, the larger the intercept, greater is the boundary layer effect. Further confirmation of the presence of intra–particle diffusion could be obtained from the existence of linear relationship between the values of the log (% removal) and log (time).

$$\text{Log (\% removal)} = c + m \log (\text{time}) \quad (11)$$

where c = intercept and m = slope

The graphs of Time vs Log C_i/C_t (Natarajan Khalaf Kinetic plot), Time vs5+Log [1–U(t)](Bhattacharya and Venkobachar kinetic plot) and Time vs2+Log (q_e-q_t) (Lagergren kinetic plot) were shown in the Figure 6. Adsorption kinetic experimental parameters on the removal ACG dye on SFPC and WFPC was shown in Table 4. The value of "r" indicates that each linear association is statistically significant. This shows that the first order of the adsorption process and these kinetic equations are applicable [26]. Among the three kinetic models, Lagergren's first-order kinetics yielded the highest 'r' value. According to this investigation, the best equation to explain the adsorption kinetics of the dye ACG on the adsorbents CAC, SFPC, and WFPC was the Lagergren first-order model.

One or more of the following processes can regulate how adsorbate is transported from the dye solution or waste water to sorbent: movie or outside dissemination: diffusion through pores: Surface diffusion is the result of multiple steps combined or adsorption on the porous surface. The possibility of intraparticle was explored by Weber-Morris intra-particle diffusion plot expresses as follows,

$$q_t = k_p t^{1/2} + C \quad \text{…….. (12)}$$

Intra-particle diffusion plot for CAC, SFPC and WFPC is shown in the Figure 7.

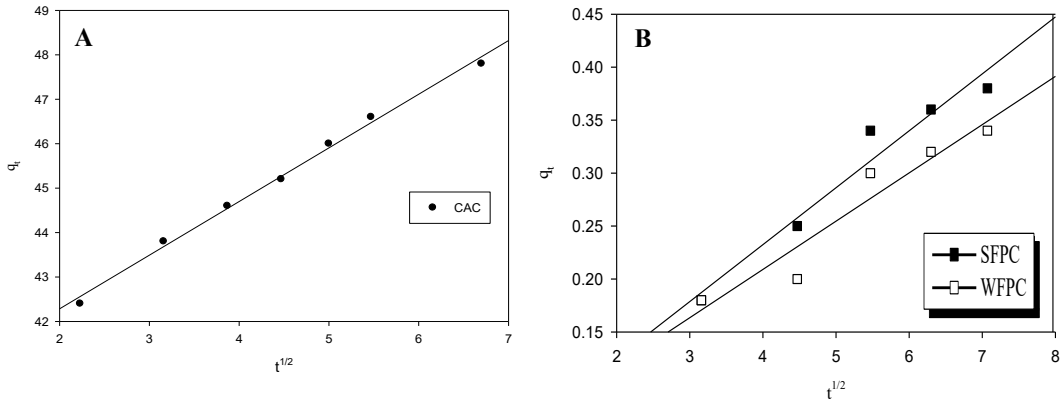

Figure 7 Intra-particle diffusion plots for ACG dye removal by adsorption on (A) CAC & (B) SFPC and WFPC

Results for Intra-particle diffusion study on the adsorption of ACG dye on CAC, SFPC and WFPC are given in Table 4. The plot of q_t against $t^{1/2}$, based on the results, gives a in a straight line in all the cases. This referred that the intra particle diffusion process controls the sorption process. The straight line's intercept and slope can be used to calculate the values of k and C. An estimate of the boundary layer's thickness can be found in the value of C. The border layer effect increases with larger intercepts [27]. The following is the order in which the intercept value and the ensuing boundary layer effect occur **CAC > SFPC > WFPC.**

3.6 Impact of weight of CAC, WFPC and SFPC adsorbents on the removal of ACG dye

The study examined the impact of adsorbent dosage at the ideal starting concentration, contact time, and pH. The percentage removal of ACG dye on various adsorbents CAC, SFPC, and WFPC are shown in Figure 8. As the adsorbent dose was raised, the proportion of dye removed rose as well. The presence of surface active sites could be the cause of this. The results indicate that an increase in the amount of ACG elimination is negligible following a dose of 2 gL^{-1} for CAC and 20 gL^{-1} for

SFPC and WFPC. Thus, 2 gL^{-1} for CAC and 20 gL^{-1} for SFPC and WFPC are set as the ideal adsorbent dosage for further or all other experimental research.

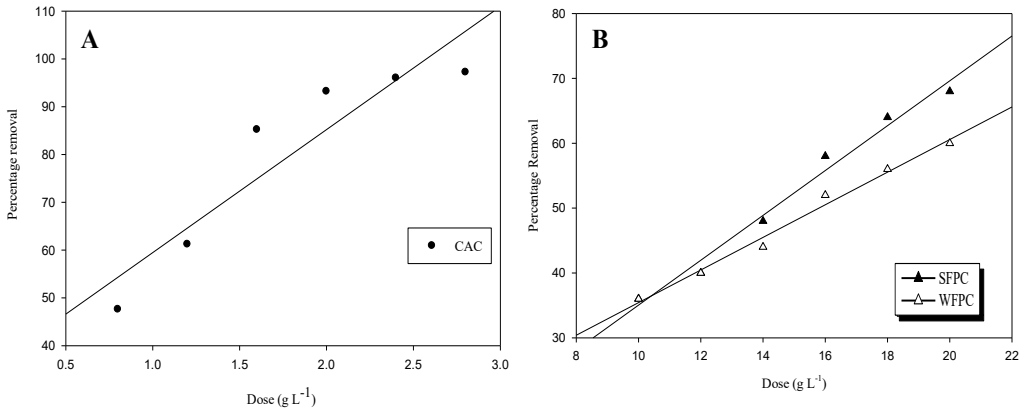

Figure 8 Effect of dose of adsorbents for the removal of MB dye due to the adsorption on (A) CAC & SFPC and WFPC [Initial concentration = 100 ppm for CAC, 10 ppm SFPC and WFPC Contact time = 30 minutes; pH = 7.5 for CAC, 6.5 for SFPC and WFPC; Particle size = 90 micron]

It was discovered that the dye's % removal vs adsorbent dose plot was exponential. Because of this, when n = fraction, the weight of dye molecules get adsorbed over these adsorbents varied according to the fractional adsorbent power term of these doses of adsorbents. This implies that the dyes that have adsorbed either obstruct the entry to interior holes to gather there, decreasing the number of active sites that are available [28-30].

3.7 Impact of pH for the elimination of ACG dye by CAC, WFPC and SFPC adsorbents

During the adsorption process, the solution pH of dye, which has a large impact on the degree of ionization, surface charge density, and adsorption capacity of the adsorbent, is important. The adsorption capacity for all the adsorbents was analyzed in the pH range 4-12 at Initial concentration = 100 ppm for CAC, 10 ppm SFPC and WFPC Contact time = 30 minutes; Dose = 2 g L^{-1} for CAC, 20 g L^{-1} for SFPC and WFPC with Particle size = 90 microns. ACG being an anionic dye has shown better adsorption at lower pH. The analysis shows that a higher percentage removal occurs in the lower pH range. This might be the result of more positive charges drawing in negatively charged dye molecules, which would increase adsorption. Diffusion and adsorption are reduced when pH rises due to de-protonation [11-13,31]. Figure 9 shows the effect of initial pH for the removal of MB dye due to the adsorption on CAC, SFPC and WFPC.

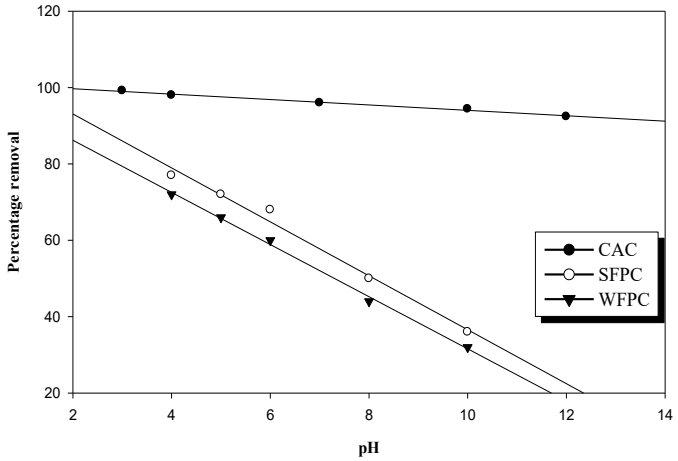

Figure 9 Effect of initial pH for the removal of MB dye due to the adsorption on CAC, SFPC and WFPC [Initial concentration = 100 ppm for CAC, 10 ppm SFPC and WFPC; Contact time = 30 minutes; Dose = 2 g L^{-1} for CAC, 20 g L^{-1} for SFPC and WFPC; Particle size = 90 micron]

The % elimination of ACG linearly increases with the decrease in initial pH for all the adsorbents (CAC, SFPC, and WFPC), which point out that the acidic pH is more suitable for the elimination of ACG dye. This study showed that the color removal of ACG is strongly influenced by the solution pH. From the observed results it is concluded that the acidic medium is favorable for removal of the ACG dye. A similar pattern was seen in how the pH shift in the solution influenced agricultural waste material's ability to remove alizarine red S from a water-based solution [33-35].

3.8 Effect of Particle Size of Adsorbents for the elimination of ACG dye on CAC, SFPC, and WFPC adsorbents

Adsorption capacity of the adsorbents CAC, SFPC and WFPC were analysed with the variation of particle size 90–300 microns and keeping all other parameters like Initial concentration = 10 ppm for SFPC and WFPC; Dose = 20 gL^{-1}; Contact time = 30 min; pH = 6.5 for SFPC and WFPC as constant. Effect of Particle size on the removal ACG dye on SFPC and WFPC adsorbents plot is given Figure 10.

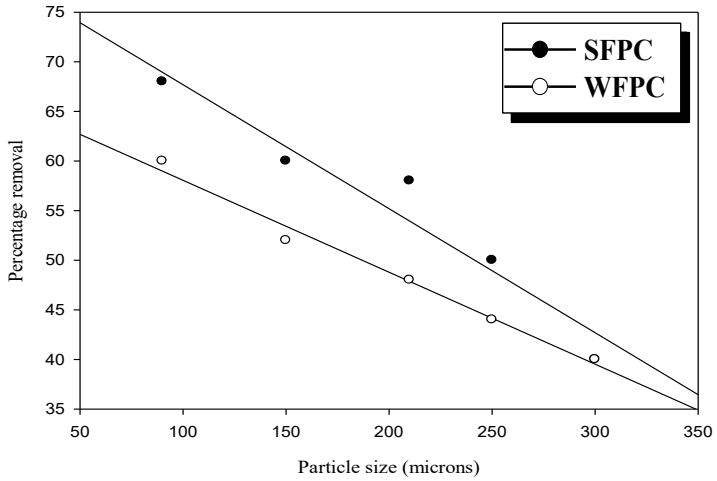

Figure 10 Effect of particle size of adsorbents for the removal of MB dye due to the adsorption on CAC, SFPC and WFPC [Initial concentration = 10 ppm for SFPC and WFPC; Dose = 20 gL^{-1}; Contact time = 30 min; pH = 6.5 for SFPC and WFPC]

The Figure 10 shows that percentage removal increases with the decrease in particle size. Therefore smaller the particle size, greater is the adsorption. Therefore smaller the particle size, the greater the adsorption. This is due to the raising the active surface area with a lower the in particle size of ACs. ACs with smaller particle sizes have higher active vacant sites and a bigger surface area, which improves sorption capacity. The distribution of particle sizes provides an approximation of the adsorbate accessible adsorbent surface area. Holes and pores on the surface of adsorbents enlarge when their surface area increase [35,36].

3.9 FT-IR analysis of MB dye before and after adsorption on IPACs

The Fourier transform infrared spectroscopy technique is an important tool for identifying characteristic functional groups which are capable of adsorbing metal ions and dye ions. FT-IR Spectral analysis was done for the adsorbents of WFPC, RFPC, MFPC and SFPC before and after sorption analysis were characterized using FT-IR spectrophotometer at room temperature. Figure 11 showed the FTIR spectral analysis of SFPC and WFPC before and after adsorption of ACG dye under optimal conditions: As seen in Figure 11, the presence of OH groups on the surface of the rice husks is confirmed by a broad band between 3300 and 3450 cm^{-1}.Here, the broad band appears at 3400.27 cm^{-1} before adsorption. After adsorption this peak shift to 3440.77 cm^{-1}.This stretching of OH groups is associated to silanol groups (Si–OH) and to adsorb water on the rice husks' surfaces. Other OH groups bound to methyl radicals exhibited a signal between 2920 and 2940 cm^{-1}. Here, the peak appeared at 2923.88 cm^{-1}.These groups are common in lignin structures. The peaks located at 1610 to 1670 cm^{-1} are characteristic of carbonyl stretching from aldehydes and ketones. Here, the peak appeared at 1612 cm^{-1} before adsorption after adsorption it appeared at 1623 cm^{-1}. The bands with the stretching between 1130–1050 and 810–800 cm^{-1} were attributed to O–Si–O and typical structures of SiO_2, which was an indication of silica. Here, the peaks appeared at1105 and 796 cm^{-1} (before adsorption) and 1107 cm^{-1} and 794 cm^{-1} (after adsorption) [37,38].

Natural Resources for Human Health
eISSN: 2583-1194

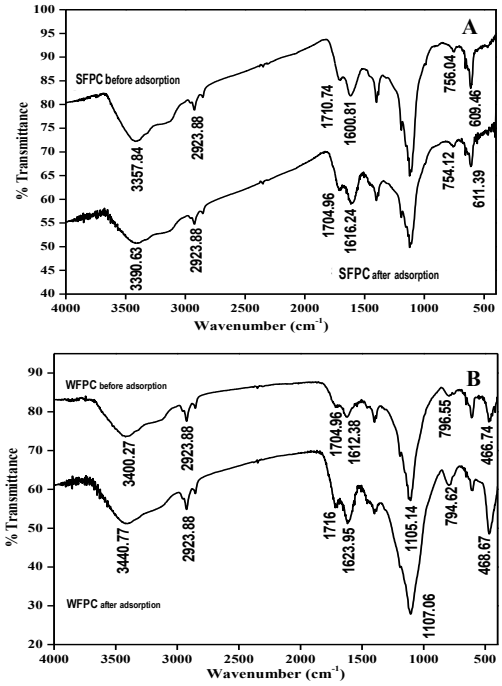

Figure 11 FT-IR Spectrum of Spectra of (A) Soursop Fruit Peel Carbon and (A) Wild Jack Fruit Peel Carbon before and after adsorption of ACG dye

3.10 Examining Surface Texture with a Scanning Electron Microscope

Studies using SEM equipments are helpful in revealing the morphological and textural features of an adsorbent's surface. Before and after dye adsorption, SEM photographs of CAC, SFPC and WFPC materials were taken. The typical SEM photographs of AC samples, before and after adsorption of dyes are shown in Figures 12.

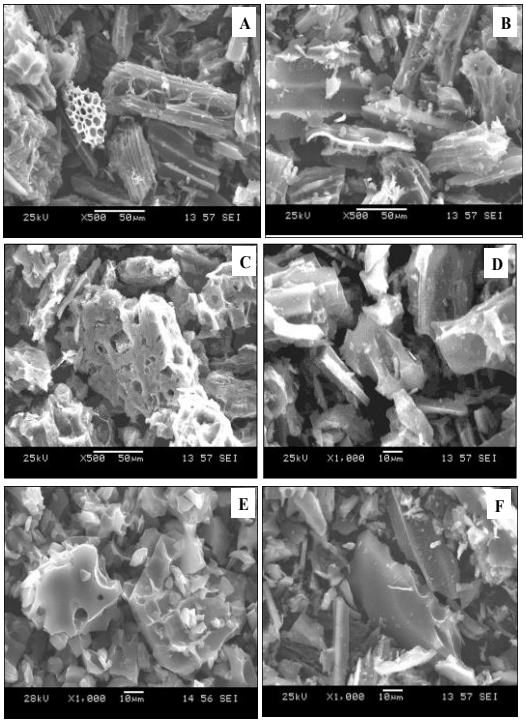

Figure 12 SEM images of CAC, SFPC and WFPC before adsoripon (A, C & E) and after adsorption (B, D & F) of ACG dye

The surface porosity and texture of the CAC and fruit peel derived carbon samples are evident in the SEM images .Furthermore, the SEM pictures show that, when the roughness factor is used to account for the defects, the particles can be informally categorized as globules or spheres. Furthermore, the globules are clearly visible and seem to be rather regular, with holes or porous structures inside of CAC and SFPC & WFPC adsorbent materials. The SEM images depicted that the particles or grains of the biomass derived activated carbon particles have interior pores (or) holes in them. The interior pores of carbonaceous materials are typically between 15 and 30 microns in size. As a result, the carbonaceous materials' porosity and graininess are clearly visualized in the SEM images. After adsorption, the porous nature of the fruit peel waste adsorbent particles either encloses or surrounds the ACG dye, which has been adsorbed on the surface. When examined under a high resolution microscope, it was discovered that activated carbons have a colour that is both black and blackish-gray, and there are also spherical particles present [39,40].

4. CONCLUSION

This research work highlighted the adsorption kinetics of the removal of dyes ACG on CAC and waste fruit peel derived SFPC and MFPC adsorbents. Batch adsorption results indicated that, when the concentration of ACG dyes solution and particle size of the adsorbent increases, the % of ACG colour removal decreases. % of ACG color removal increases with increasing in agitation time and dose of adsorbents. The % of color removal strongly depends on the nature of the dye solution. ACG is a anionic dye, so the color removal increases with and decrease in pH. The equilibrium data fitted well with Langmuir and Freundlich isotherm models, indicating the feasibility of monolayer and heterogeneous surface adsorption. The value of Q0 is in the order: CAC > SFPC > WFPC. The kinetics of adsorption follows pseudo-second-order showing that the nature of sorption is controlled by chemisorption. In conclusion, fruit peel derived carbons exhibited promising adsorption performance, demonstrating their potential as low-cost, eco-friendly materials alternate to CAC for wastewater treatment applications.

ACKNOWLEDGEMENTS

Authors acknowledge the Management and Principal of Women's Christian College, Nagercoil for providing Research facility.

AUTHOR CONTRIBUTIONS

Maheswari M: conceptualization, methodology, data analysis, manuscript writing, and editing.

Muthirulan P: funding acquisition, resources, supervision, proofreading, editing.

Starlin Kamala C: methodology, proofreading, editing and resources.

CONFLICT OF INTEREST

The authors declare that there is no conflict of interest.

ETHICS STATEMENT

Ethical approval was not required for this study.

DATA AVAILABILITY STATEMENT

Data supporting the findings of this study are available from the corresponding author upon reasonable request.

REFERENCES

[1] Yeow, P.K., Wong, S.W., Hadibarata, T., 2021. Removal of Azo and Anthraquinone Dye by Plant Biomass as Adsorbent – A Review. Biointerface Research in Applied Chemistry 11, 8218–8232.

[2] Rahimian, R., Zarinabadi, S., 2020. A Review of Studies on the Removal of Methylene Blue Dye from Industrial Wastewater Using Activated Carbon Adsorbents Made from Almond Bark. Progress in Chemical and Biochemical Research 3, 251–268.

[3] Hassan, M.M., Carr, C.M., 2021. Biomass-derived Porous Carbonaceous Materials and Their Composites as Adsorbents for Cationic and Anionic Dyes: A Review. Chemosphere 265, 129087.

[4] Bulgariu, L., Escudero, L.B., Bello, O.S., Iqbal, M., Nisar, J., Adegoke, K.A., 2019. The Utilization of Leaf-Based Adsorbents for Dyes Removal: A Review. Journal of Molecular Liquids 276, 728–747.

[5] Shaikhiev, I.G., Kraysman, N.V., Sverguzova, S.V., 2021. Review of almond (Prunus dulcis) shell use to remove pollutants from aquatic environments. Biointerface Research in Applied Chemistry 11, 14866–14880.

[6] Al-Tohamy, R., Ali, S.S., Li, F., et al., 2022. A critical review on the treatment of dye-containing wastewater: ecotoxicological and health concerns of textile dyes and possible remediation approaches for environmental safety. Ecotoxicology and Environmental Safety 231, 113160.

[7] Fouda-Mbanga, B.G., Onotu, O.P., Tywabi-Ngeva, Z., 2024. Advantages of the reuse of spent adsorbents and potential applications in environmental remediation: a review. Green Analytical Chemistry 11, 100156.

[8] Yaseen, D.A., Scholz, M., 2019. Textile dye wastewater characteristics and constituents of synthetic effluents: a critical review. International Journal of Environmental Science and Technology 16, 1193–1226.

[9] Escudero-Curiel, S., Giráldez, A., Pazos, M., Sanromán, Á., 2023. From waste to resource: valorization of lignocellulosic agri-food residues through engineered hydrochar and biochar for environmental and clean energy applications—a comprehensive review. Foods 12, 3646.

[10] Mkilima, T., Zharkenov, Y., Abduova, A., et al., 2024. Utilization of banana peel-derived activated carbon for the removal of heavy metals from industrial wastewater. Case Studies in Chemical and Environmental Engineering 10, 100791.

[11] Shahul Hameed, K., Muthirulan, P., Meenakshi, S.M., 2017. Adsorption of chromotrope dye onto activated carbons obtained from the seeds of various plants: equilibrium and kinetics studies. Arabian Journal of Chemistry 10, S2225–S2233.

[12] Kannan, N., Meenakshi, S.M., 2001. Kinetics and mechanism of removal of methylene blue by adsorption on various carbons – a comparative study. Dyes and Pigments 51, 25–40.

[13] Ramaraj, R., Shanmugam, A., Nagarathinam, B., et al., 2023. Agriculture byproduct-derived versatile Cassia fistula seed shell carbon for the removal of acid violet 17 dye from aqueous solution: adsorption kinetics, equilibrium, and mechanism studies. Biomass Conversion and Biorefinery 13, 9507–9523.

[14] Ajemba, R.O., 2014. Adsorption of Malachite green from aqueous solution using activated Ntezi clay: optimization, isotherm and kinetic studies. International Journal of Engineering 27(6), 839–854.

[15] Karim, M.A., Ahmed, S., Hossain, D., Hossain, M.I., Hossain, M.S., Hossain, A., Rahman, M.H., Dipti, S.S., Azad, M.A.K., 2024. Adsorption isotherm and kinetics studies on adsorption of malachite green onto activated charcoal from aqueous solution. Journal of Science and Engineering Papers 1(1), 18–25.

[16] Ali, A.F., Kovo, A.S., Adetunji, S.A., 2017. Methylene blue and brilliant green dyes removal from aqueous solution using agricultural wastes activated carbon. Journal of Encapsulation and Adsorption Sciences 7(2), 95–107.

[17] Laskar, N., Kumar, U., 2019. Removal of Brilliant Green dye from water by modified Bambusa Tulda: adsorption isotherm, kinetics and thermodynamics study. International Journal of Environmental Science and Technology 16, 1649–1662.

[18] Karim, M.A., Najibullah, M., Ahmed, S., et al., 2025. Adsorption isotherms studied on synthesized corn cob-based activated carbon as an adsorbent for removal of methyl orange dye from aqueous solution. Biomass Conversion and Biorefinery 15, 24149–24168.

[19] Kocabiyik, B., Bayrak, Y., 2024. Application of a Bio-waste Einkorn (Triticum monococcum L.) Husks Adsorbent for Removal of Metanil Yellow and Methylene Blue from Aqueous Media with Equilibrium, Kinetic, and Thermodynamic Studies. Water, Air, & Soil Pollution 235, 200.

[20] Gujar, J.P., Gautam, M.K., Modhera, B., 2025. Valorization of banana peel into activated carbon for efficient and sustainable dye removal in textile industry. Biomass Conversion and Biorefinery 15, 29363–29382.

[21] Reddy, Y.S., Jose, T.J., Dinesh, B., et al., 2025. Equilibrium, kinetic, and thermodynamic study of Direct Yellow 12 dye adsorption by biomass-derived porous graphitic activated carbon. Biomass Conversion and Biorefinery 15, 6817–6833.

[22] Senapati, S., Giri, J., Mallick, L., et al., 2025. Ultra-fast adsorption of the industrial cationic dye pollutant using nitric acid-activated rice straw biochar: insights into adsorption mechanisms. Biomass Conversion and Biorefinery 15, 18905–18923.

[23] Crespo, L.H.S., Dutra, L.P., Andrade, A.A.R., et al., 2025. Comparative study of the adsorption mechanisms of caffeine and Remazol brilliant blue R dye on activated carbon from alpaca fiber residue. Biomass Conversion and Biorefinery 15, 25307–25322.

[24] Abate, G.Y., Alene, A.N., Habte, A.T., et al., 2020. Adsorptive removal of malachite green dye from aqueous solution onto activated carbon of Catha edulis stem as a low cost bio-adsorbent. Environmental Systems Research 9, 29.

[25] Mohamad, S., Muslum, D., Kuok, H.D.T., Linh, T.T., Seng, B., Chen, T.-W., Noura, M.D., Bandar, M.A., Tony, H., 2022. Removal of Cresol Red by Adsorption Using Wastepaper. Industrial and Domestic Waste Management 2(1), 1–8.

[26] Bouhadjra, K., Lemlikchi, W., Ferhati, A., Mignard, S., 2021. Enhancing Removal Efficiency of Anionic Dye (Cibacron Blue) Using Waste Potato Peels Powder. Scientific Reports 11, 1–10.

[27] Bustos-Terrones, Y.A., Hermosillo-Nevárez, J.J., Ramírez-Pereda, B., Vaca, M., Rangel-Peraza, J.G., Bustos-Terrones, V., 2021. Removal of BB9 Textile Dye by Biological, Physical, Chemical, and Electrochemical Treatments. Journal of the Taiwan Institute of Chemical Engineers 121, 29–37.

[28] Sujesh, S., Gokulakrishnan, M., Thivaharan, V., Ramesh, V., Raja, S., 2025. Efficient adsorptive removal of Congo Red dye using activated carbon derived from Spathodea campanulata flowers. Scientific Reports 15, 1831.

[29] Heidarinejad, Z., Dehghani, M.H., Heidari, M., Javedan, G., Ali, I., Sillanpää, M., 2020. Methods for Preparation and Activation of Activated Carbon: A Review. Environmental Chemistry Letters 18, 393–415.

[30] Jawad, A.H., Mohd Firdaus Hum, N.N., Abdulhameed, A.S., Mohd Ishak, M.A., 2020. Mesoporous Activated Carbon from Grass Waste via H3PO4-Activation for Methylene Blue Dye Removal: Modelling, Optimisation, and Mechanism Study. International Journal of Environmental Analytical Chemistry, 1–17.

[31] Mohd Nasir, M.Z., Indiran, G., Ahmad Zaini, M.A., 2021. Assessment of thermal regeneration of spent commercial activated carbon for methylene blue dye removal. Particulate Science and Technology 39, 504–510.

[32] Talbachew Tadesse Nadew, Mestawot Keana, Tsegaye Sisay, Belay Getye, Nigus Gabbiye Habtu, 2023. Synthesis of activated carbon from banana peels for dye removal of an aqueous solution in textile industries: optimization, kinetics, and isotherm aspects. Water Practice and Technology 18(4), 947–966.

[33] Bazan-Wozniak, A., Jędrzejczak, A., Wolski, R., Kaczmarek, S., Nosal-Wiercińska, A., Cielecka-Piontek, J., Yagmur-Kabas, S., Pietrzak, R., 2024. A Study on the Adsorption of Rhodamine B onto Adsorbents Prepared from Low-Carbon Fossils: Kinetic, Isotherm, and Thermodynamic Analyses. Molecules 29(6), 1412.

[34] Bazan-Wozniak, A., Wolski, R., Paluch, D., Nowicki, P., Pietrzak, R., 2022. Removal of Organic Dyes from Aqueous Solutions by Activated Carbons Prepared from Residue of Supercritical Extraction of Marigold. Materials 15(10), 3655.

[35] Seyedi, Z.S., Zahraei, Z., Jookar Kashi, F., 2020. Decolorization of Reactive Black 5 and Reactive Red 152 Azo Dyes by New Haloalkaliphilic Bacteria Isolated from the Textile Wastewater. Current Microbiology 77, 2084–2092.

[36] Prasad, B., Goswami, R., Mishra, A., 2024. Assessment of carbonized Himalayan chir pine biomass as an eco-friendly adsorbent for effective removal of industrial dyes. Scientific Reports 14, 15694.

[37] Yu, K.L., Lee, X.J., Ong, H.C., Chen, W.H., Chang, J., Lin, C.S., 2021. Adsorptive Removal of Cationic Methylene Blue and Anionic Congo Red Dyes Using Wet-Torrefied Microalgal Biochar: Equilibrium, Kinetic and Mechanism Modeling. Environmental Pollution 272, 115986.

[38] Yang, Z., Hou, J., Miao, L., Wu, J., 2021. Comparison of Adsorption Behavior Studies of Methylene Blue by Microalga Residue and its Biochars Produced at Different Pyrolytic Temperatures. Environmental Science and Pollution Research 28, 14028–14040.

[39] Ramaraj, R., Nagarathinam, B., Pandi, M., 2023. Biomass-derived activated porous carbon from Manilkara kauki L. bark as potential adsorbent for the removal of Congo red dye from aqueous solution. Biomass Conversion and Biorefinery 13, 9475–9485.

[40] Sivakumar, S., Muthirulan, P., Meenakshi Sundaram, M., 2019. Adsorption kinetic and isotherm studies of Azure A on various activated carbons derived from agricultural wastes. Arabian Journal of Chemistry 12, 1507–1514.